



Supplement of

Simulating the SOA formation of isoprene from partitioning and aerosol phase reactions in the presence of inorganics

R. L. Beardsley and M. Jang

Correspondence to: M. Jang (mjang@ufl.edu)

The copyright of individual parts of the supplement might differ from the CC-BY 3.0 licence.

Section S1: Gas phase simulations and lumping

Gas phase oxidation. The Master Chemical Mechanism v3.2 (Saunders et al., 1997, 2003) was employed within the Morpho Kinetic Solver (Jeffries, H.E. et al., 1998) to simulate isoprene photooxidation for the range of VOC/NO_x shown in Table S1. The simulations were run using the temperature (T), relative humidity (RH) and total ultra-violet radiation (UV) data measured on 23 April 2014 measured in the UF APHOR chamber (Figure S1). Then, the predicted gas phase concentrations of each species at the maximum HO₂/NO were used for lumping as a function of VOC/NO_x.

Table S1. Concentrations of isoprene and NO_x used in gas phase photooxidation simulations of isoprene used in lumping as a function of VOC/NO_x

ISO (ppb)	500	500	500	500	500	500	500	500	500	500	500
NO _x (ppb)	25	40	50	75	100	150	200	300	400	500	625
VOC/NO_x (ppbC/ppb)	100	62.5	50	33.33	25	16.67	12.5	8.33	6.25	5	4

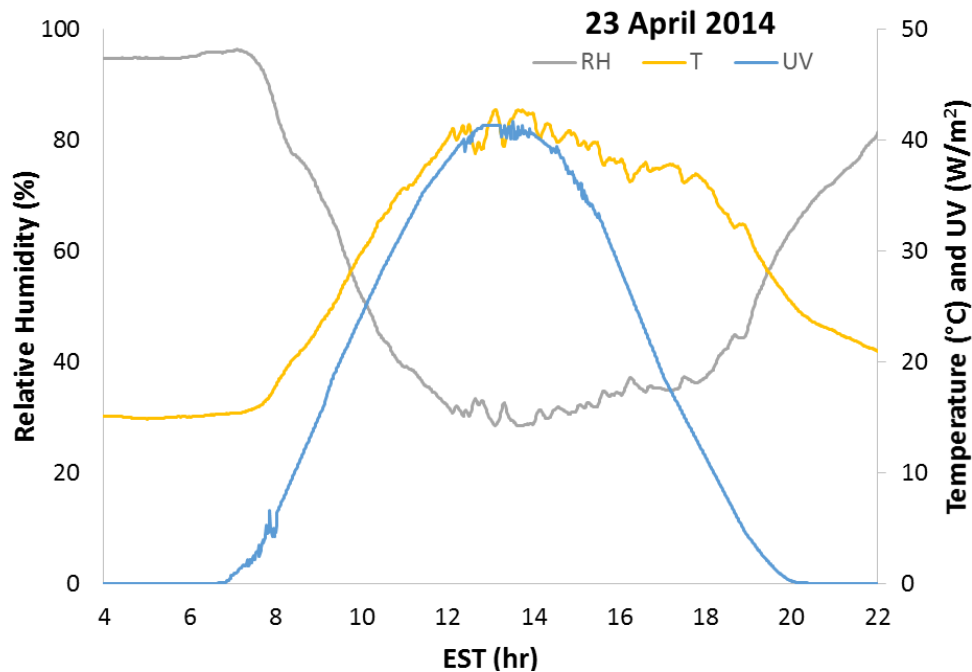


Figure S1. Time profile of relative humidity, temperature, and total ultra-violet radiation measured in the UF-APHOR chambers on 23 April 2014.

MCM and Morpho were also used to provide the ΔISO required by UNIPAR for each experimental simulation. It was determined that the MCM is reasonably representative of the actual photooxidation by comparing the measured and predicted concentrations of isoprene, NO, NO_2 and O_3 in each experiment. Figure S2 shows the measured and modeled concentrations from the east chamber of experiment A on 27 January 2015 as an example. The major discrepancies in each simulation occur between the model and experimental values for O_3 and NO_2 as can be seen in Fig. S2. MCM predicts a higher O_3 concentration than reality and that it forms more quickly. On the other hand, while the predicted and measured peak NO_2 match reasonably well the measured NO_2 is higher than the predicted late in the experiment. This is likely due to organonitrates being detected as NO_2 by the chemiluminescence NO_x analyzer.

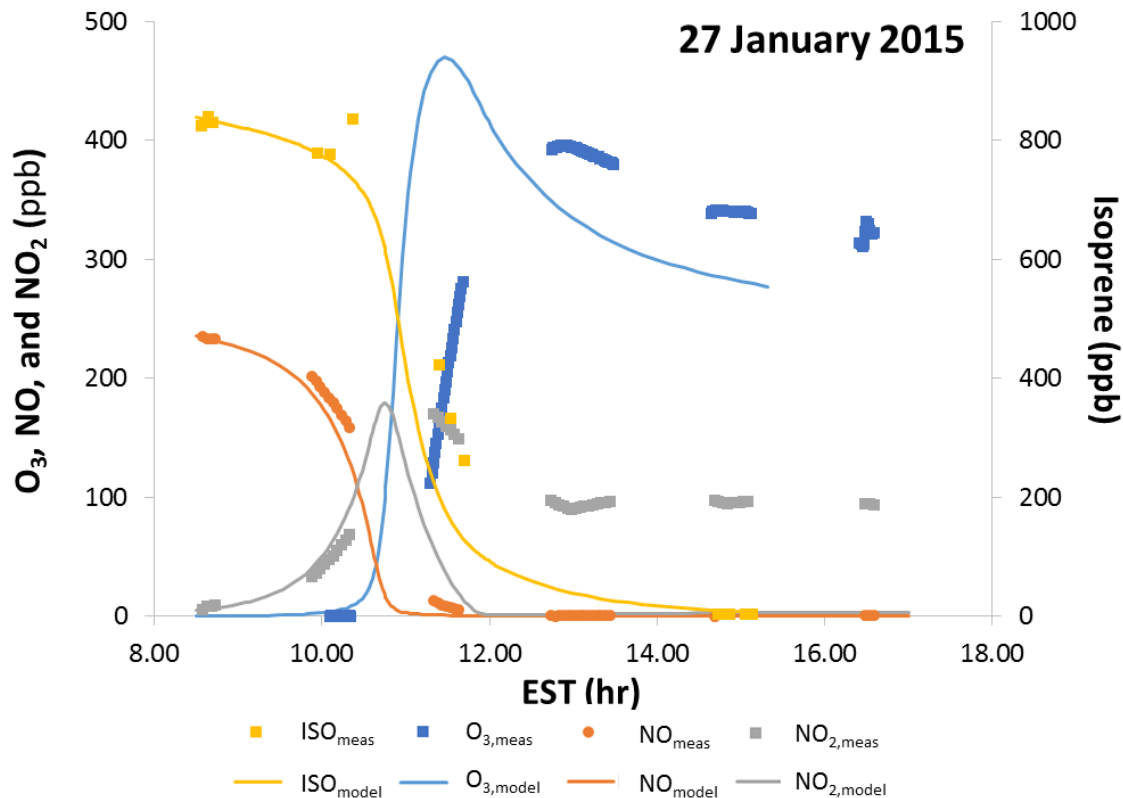


Figure S2. Time profile of the measured and predicted isoprene, NO, NO_2 , and O_3 from 27 January, 2015 in the east UF-APHOR chamber.

Lumping. As is described in detail in Sect. 3.1, the products from MCM are lumped based on their vapor pressure and reactivity in aerosol phase reactions. Figure S3 shows the product of highest concentration in each lumping group when VOC/NO_x is 25. The empty groups are those for which isoprene has no photooxidation products.

$\alpha_{m,n}$	Vapor Pressure (mmHg) [n]						
	n = 1 (10 ⁻⁸)	n = 2 (10 ⁻⁶)	n = 3 (10 ⁻⁵)	n = 4 (10 ⁻⁴)	n = 5 (10 ⁻³)	n = 6 (10 ⁻²)	n = 7 (10 ⁻¹)
VF							
F							
M							
S							
P							
OSp							
IEPOX							

Figure S3. The lumping structure of UNIPAR filled with the product of highest concentration in each lumping group at a VOC/NO_x of 25. Empty bins represent lumping groups for which isoprene has no photooxidation products.

Section S2: Estimation of aerosol acidity($[H^+]$)

In UNIPAR, the aerosol liquid water content (LWC) and acidity ($[H^+]$) are predicted using the inorganic thermodynamic model E-AIM II (Clegg et al., 1998) as a function of $[SO_4^{2-}]$ and $[NH_4^+]$, corrected for the ammonia rich condition based on the results of Li and Jang (2012). Since isoprene are SHMP SOA, the interaction of organics and inorganics in the mixed phase may influence the dissociation of inorganic acids potentially leading to large deviations from the predicted $[H^+]$. AIOMFAC was employed to determine whether not this influence is significant. Table S2 shows the fractional dissociation of H_2SO_4 in the presence of varying amounts of tetrol and hexane, which represent polar and non-polar organic species. Although there is a reduction in the dissociation of sulfuric acid due to the presence of both tetrol and hexane, the maximum percent difference in these simulations is less than 12%. Based on these results, it was assumed that protonation is not significantly impacted by the presence of organics, and the $[H^+]$ predicted by the inorganic composition is simply diluted by the concentration of organics in each time step. This assumption introduces uncertainty into the prediction of aerosol phase reactions, but there is not currently an approach with little uncertainty to predict $[H^+]$ of mixed inorganic/organic aerosol composed of a large number of species.

Table S2. Output from AIOMFAC simulations performed to determine the impact of the presence of organics on the protonation of sulfuric acid. Tetrol and hexane were used to represent polar and non-polar organics.

organic	RH(%)	X_{org}	X_{H^+}	X_{SO_4}	X_{HSO_4}	$H/(H+SO_4+HSO_4)$
tetrol	46.35	0.000	0.150	0.039	0.072	0.575
tetrol	44.04	0.194	0.120	0.005	0.110	0.510
tetrol	47.66	0.114	0.125	0.011	0.103	0.523
tetrol	20.06	0.000	0.202	0.042	0.118	0.558
tetrol	20.51	0.366	0.169	0.003	0.164	0.504
tetrol	19.71	0.204	0.216	0.012	0.192	0.514
hexane	49.98	0.000	0.143	0.038	0.067	0.577
hexane	51.98	0.210	0.125	0.018	0.090	0.538
hexane	50.97	0.089	0.114	0.026	0.063	0.563
hexane	20.06	0.000	0.202	0.042	0.118	0.558
hexane	21.05	0.204	0.203	0.008	0.187	0.510
hexane	22.56	0.382	0.185	0.022	0.141	0.531

Section S3: Prediction of the activity coefficients of organic species in SHMP isoprene SOA

As is described in Sect 3.3 of the manuscript, the non-ideality of each lumping species in the SHMP aerosol is accounted for by the activity coefficient $\gamma_{mix,i}$. $\gamma_{mix,i}$ will vary between each species due to differences in polarity and molar volume, and over time due to changes in aerosol phase composition. In order to estimate $\gamma_{mix,i}$ for the lumped isoprene photooxidation products,

AIOMFAC was run for the highest concentration product of each lumping group in the presence

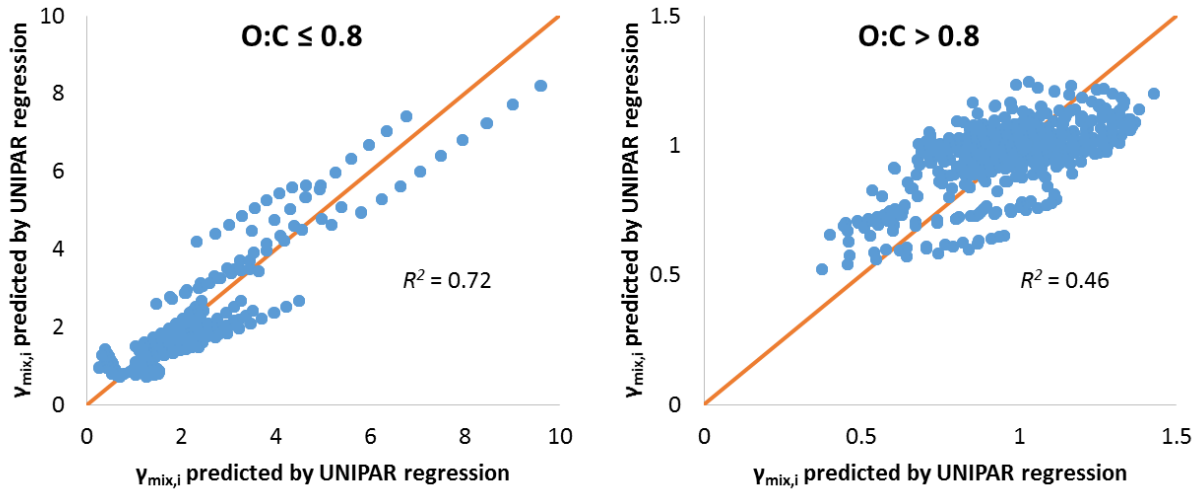


Figure S4. The $\gamma_{mix,i}$ predicted by AIOMFAC plotted against the $\gamma_{mix,i}$ predicted by the regressions in Eq. S1 and S2 along with a $y=x$ line and the R^2 .

of a mixed isoprene SOA-ammonium sulfate aerosol with the SOA composition based on the results of Nguyen et al. (2011). The bulk organic to sulfur mass ratio (org:sulf), concentration of i , and RH were varied to cover the range of experimental values. The resulting $\gamma_{mix,i}$ were fit to the bulk org:sulf, $\ln(RH)$, the oxygen to carbon molar ratio ($O:C_i$) of i and molar volume($V_{mol,i}$) of i for two ranges of O:C. The parameterizations are shown in equations S1 and S2 below.

O:C ≤ 0.8

$$\ln(\gamma_{mix,i}) = 2.354 + 0.146 * \ln(RH) + 0.128 * org : sulf - 3.195 * O : C \quad (S1)$$

O:C > 0.8

$$\ln(\gamma_{mix,i}) = -0.229 + 0.050 * \ln(RH) - 0.011 * org : sulf - 0.252 * O : C + 0.007 * V_{mol,i} \quad (S2)$$

The regressions for $\gamma_{mix,i}$ have R^2 of 0.72 and 0.46 for O:C less than or equal to 0.8 and greater than 0.8, respectively, as is shown in Figure S4. The polar compounds used in fitting Eq S1 have

AIOMFAC predicted $\gamma_{mix,i}$ that range from 0.5 to 5.5, while those of O:C greater than 0.8 only range from 0.5 to 1.5. The small range of $\gamma_{mix,i}$ for Eq. S2 leads to higher residuals and a lower R^2 , but all of the values predicted by AIOMFAC and the regressions generated are close to unity minimizing the impact of error on model output.

Section S4. Concentration of isoprene SOA products as a function of VOC/NO_x

In both the simulated and experimental SOA formation of isoprene, there is an increase in SOA yield with increasing NO_x (decreasing VOC/NO_x), and the influence of NO_x is stronger in the presence of acidity. The mass stoichiometric coefficients of products that contribute significantly

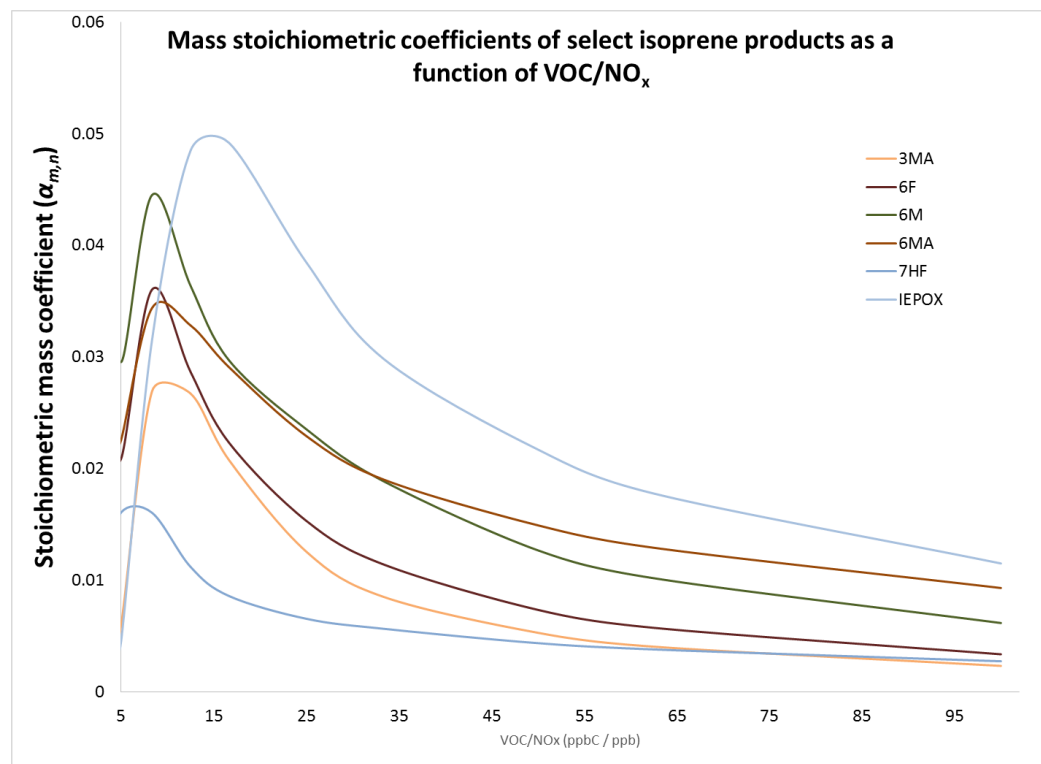


Figure S5. The stoichiometric mass coefficients ($\alpha_{m,n}$) of selected products which contribute significantly to isoprene SOA as a function of VOC/NO_x.

to the simulated isoprene SOA are shown in Figure S5 below. The stoichiometric coefficients are calculated using simulations based on the Master Chemical Mechanism within the Morpho Kinetic Solver (Sect. S1). As can be seen, all of the products are lower in concentration with a reduction in NO_x under the conditions of this study (VOC/NO_x: 10 to 100). The reduction in products that are highly reactive in aerosol phase reactions, such as glyoxal (6F, in Figure S5) explains the increased sensitivity to VOC/NO_x in the presence of acidic seed.

Section S5. Model Sensitivity and Uncertainty

In order to determine the impact of the uncertainty of the underlying modules and parameterizations applied in UNIPAR, sensitivity tests were performed in which vapor pressure ($p_{L,i}^o$), enthalpy of vaporization ($\Delta H_{vap,i}$), activity coefficient of i in the SHMP aerosol ($\gamma_{mix,i}$), and the aerosol phase reaction rate of i ($k_{AR,i}$) were increased and decreased by a factor chosen to exceed the possible error of the method. After applying the factors, simulations of Exp. SA1 were performed and the resulting percent change in OM_T is shown in Figure S5.

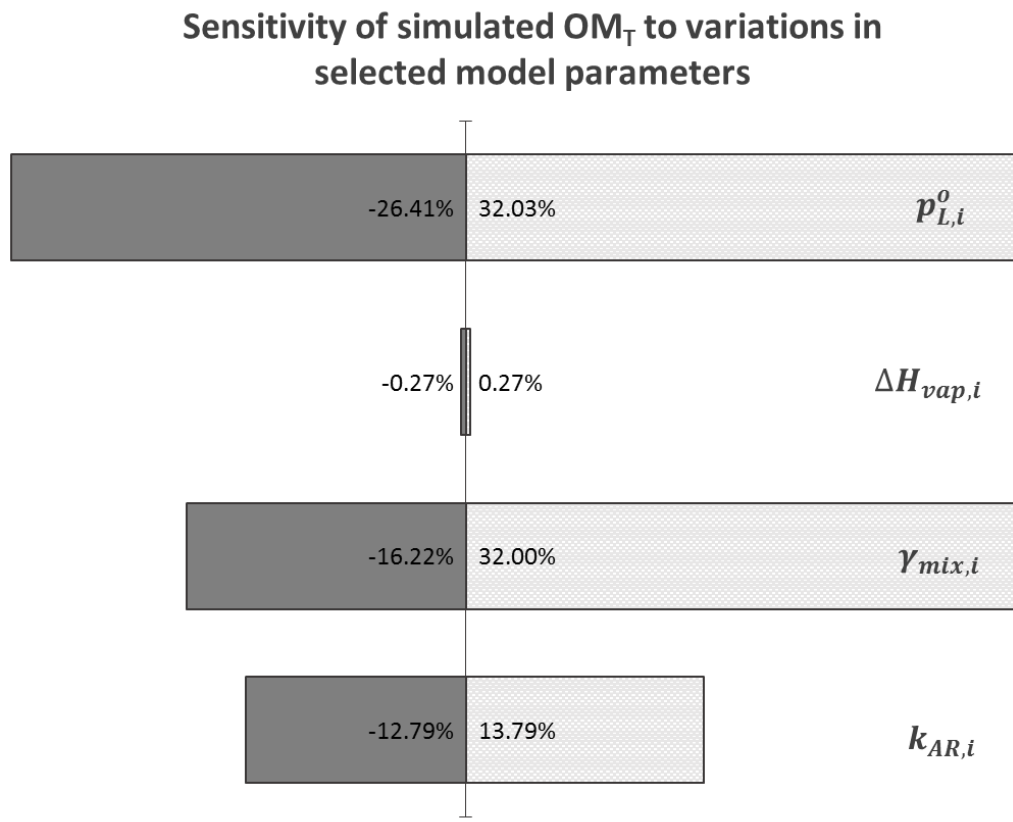


Figure S6. The percent change in the model predicted OM_T from experiment SA1 after each parameter was increased and decreased by a factor chosen to exceed the uncertainty of the underlying methods used for estimating each variable.

References:

Clegg, S. L., Brimblecombe, P. and Wexler, A. S.: Thermodynamic Model of the System H+-NH4+-SO42--NO3--H2O at Tropospheric Temperatures, *J. Phys. Chem. A*, 102(12), 2137–2154, doi:10.1021/jp973042r, 1998.

Jeffries, H.E., Gary, M. W., Kessler, M and Sexton, K. G.: Morphecule reaction mechanism, *Morpho.*, 1998.

Li, J. and Jang, M.: Aerosol Acidity Measurement Using Colorimetry Coupled With a Reflectance UV-Visible Spectrometer, *Aerosol Sci. Technol.*, 46(8), 833–842, doi:10.1080/02786826.2012.669873, 2012.

Nguyen, T. B., Roach, P. J., Laskin, J., Laskin, A. and Nizkorodov, S. A.: Effect of humidity on the composition of isoprene photooxidation secondary organic aerosol, *Atmos Chem Phys*, 11(14), 6931–6944, doi:10.5194/acp-11-6931-2011, 2011.

Saunders, S. M., Jenkin, M. E., Derwent, R. G. and Pilling, M. J.: World wide web site of a master chemical mechanism (MCM) for use in tropospheric chemistry models, *Atmospheric Environ. - ATMOS Env.*, 31(8), 1249–1249, doi:10.1016/S1352-2310(97)85197-7, 1997.

Saunders, S. M., Jenkin, M. E., Derwent, R. G. and Pilling, M. J.: Protocol for the development of the Master Chemical Mechanism, MCM v3 (Part A): tropospheric degradation of non-aromatic volatile organic compounds, *Atmos Chem Phys*, 3(1), 161–180, doi:10.5194/acp-3-161-2003, 2003.